

Search for Randall-Sundrum gravitons in the dielectron and diphoton final states with 5.4 fb^{-1} of data from $p\bar{p}$ collisions at $\sqrt{s} = 1.96 \text{ TeV}$

V.M. Abazov³⁶, B. Abbott⁷⁴, M. Abolins⁶³, B.S. Acharya²⁹, M. Adams⁴⁹, T. Adams⁴⁷, E. Aguilo⁶, G.D. Alexeev³⁶, G. Alkhazov⁴⁰, A. Alton^{62,a}, G. Alverson⁶¹, G.A. Alves², L.S. Ancu³⁵, M. Aoki⁴⁸, Y. Arnaud¹⁴, M. Arov⁵⁸, A. Askew⁴⁷, B. Åsman⁴¹, O. Atramentov⁶⁶, C. Avila⁸, J. BackusMayes⁸¹, F. Badaud¹³, L. Bagby⁴⁸, B. Baldin⁴⁸, D.V. Bandurin⁴⁷, S. Banerjee²⁹, E. Barberis⁶¹, A.-F. Barfuss¹⁵, P. Baringer⁵⁶, J. Barreto², J.F. Bartlett⁴⁸, U. Bassler¹⁸, S. Beale⁶, A. Bean⁵⁶, M. Begalli³, M. Begel⁷², C. Belanger-Champagne⁴¹, L. Bellantoni⁴⁸, J.A. Benitez⁶³, S.B. Beri²⁷, G. Bernardi¹⁷, R. Bernhard²², I. Bertram⁴², M. Besançon¹⁸, R. Beuselinck⁴³, V.A. Bezzubov³⁹, P.C. Bhat⁴⁸, V. Bhatnagar²⁷, G. Blazey⁵⁰, S. Blessing⁴⁷, K. Bloom⁶⁵, A. Boehnlein⁴⁸, D. Boline⁷¹, T.A. Bolton⁵⁷, E.E. Boos³⁸, G. Borisso⁴², T. Bose⁶⁰, A. Brandt⁷⁷, R. Brock⁶³, G. Brooijmans⁶⁹, A. Bross⁴⁸, D. Brown¹⁹, X.B. Bu⁷, D. Buchholz⁵¹, M. Buehler⁸⁰, V. Buescher²⁴, V. Bunichev³⁸, S. Burdin^{42,b}, T.H. Burnett⁸¹, C.P. Buszello⁴³, P. Calfayan²⁵, B. Calpas¹⁵, S. Calvet¹⁶, E. Camacho-Pérez³³, J. Cammin⁷⁰, M.A. Carrasco-Lizarraga³³, E. Carrera⁴⁷, B.C.K. Casey⁴⁸, H. Castilla-Valdez³³, S. Chakrabarti⁷¹, D. Chakraborty⁵⁰, K.M. Chan⁵⁴, A. Chandra⁷⁹, G. Chen⁵⁶, S. Chevalier-Théry¹⁸, D.K. Cho⁷⁶, S.W. Cho³¹, S. Choi³², B. Choudhary²⁸, T. Christoudias⁴³, S. Cihangir⁴⁸, D. Claes⁶⁵, J. Clutter⁵⁶, M.S. Cooke⁶⁹, M. Cooke⁴⁸, W.E. Cooper⁴⁸, M. Corcoran⁷⁹, F. Couderc¹⁸, M.-C. Cousinou¹⁵, A. Croc¹⁸, D. Cutts⁷⁶, M. Ćwiok³⁰, A. Das⁴⁵, G. Davies⁴³, K. De⁷⁷, S.J. de Jong³⁵, E. De La Cruz-Burelo³³, K. DeVaughan⁶⁵, F. Déliot¹⁸, M. Demarteau⁴⁸, R. Demina⁷⁰, D. Denisov⁴⁸, S.P. Denisov³⁹, S. Desai⁴⁸, H.T. Diehl⁴⁸, M. Diesburg⁴⁸, A. Dominguez⁶⁵, T. Dorland⁸¹, A. Dubey²⁸, L.V. Dudko³⁸, D. Duggan⁶⁶, A. Duperrin¹⁵, S. Dutt²⁷, A. Dyshkant⁵⁰, M. Eads⁶⁵, D. Edmunds⁶³, J. Ellison⁴⁶, V.D. Elvira⁴⁸, Y. Enari¹⁷, S. Eno⁵⁹, H. Evans⁵², A. Evdokimov⁷², V.N. Evdokimov³⁹, G. Facini⁶¹, A.V. Ferapontov⁷⁶, T. Ferbel^{59,70}, F. Fiedler²⁴, F. Filthaut³⁵, W. Fisher⁶³, H.E. Fisk⁴⁸, M. Fortner⁵⁰, H. Fox⁴², S. Fuess⁴⁸, T. Gadfort⁷², A. Garcia-Bellido⁷⁰, V. Gavrilov³⁷, P. Gay¹³, W. Geist¹⁹, W. Geng^{15,63}, D. Gerbaudo⁶⁷, C.E. Gerber⁴⁹, Y. Gershtein⁶⁶, D. Gillberg⁶, G. Ginther^{48,70}, G. Golovanov³⁶, A. Goussiou⁸¹, P.D. Grannis⁷¹, S. Greder¹⁹, H. Greenlee⁴⁸, Z.D. Greenwood⁵⁸, E.M. Gregores⁴, G. Grenier²⁰, Ph. Gris¹³, J.-F. Grivaz¹⁶, A. Grohsjean¹⁸, S. Grünendahl⁴⁸, M.W. Grünewald³⁰, F. Guo⁷¹, J. Guo⁷¹, G. Gutierrez⁴⁸, P. Gutierrez⁷⁴, A. Haas^{69,c}, P. Haefner²⁵, S. Hagopian⁴⁷, J. Haley⁶¹, I. Hall⁶³, L. Han⁷, K. Harder⁴⁴, A. Harel⁷⁰, J.M. Hauptman⁵⁵, J. Hays⁴³, T. Hebbeker²¹, D. Hedin⁵⁰, A.P. Heinson⁴⁶, U. Heintz⁷⁶, C. Hensel²³, I. Heredia-De La Cruz³³, K. Herner⁶², G. Hesketh⁶¹, M.D. Hildreth⁵⁴, R. Hirosky⁸⁰, T. Hoang⁴⁷, J.D. Hobbs⁷¹, B. Hoeneisen¹², M. Hohlfeld²⁴, S. Hossain⁷⁴, P. Houben³⁴, Y. Hu⁷¹, Z. Hubacek¹⁰, N. Huske¹⁷, V. Hynek¹⁰, I. Iashvili⁶⁸, R. Illingworth⁴⁸, A.S. Ito⁴⁸, S. Jabeen⁷⁶, M. Jaffré¹⁶, S. Jain⁶⁸, D. Jamin¹⁵, R. Jesik⁴³, K. Johns⁴⁵, C. Johnson⁶⁹, M. Johnson⁴⁸, D. Johnston⁶⁵, A. Jonckheere⁴⁸, P. Jonsson⁴³, A. Juste^{48,d}, K. Kaadze⁵⁷, E. Kajfasz¹⁵, D. Karmanov³⁸, P.A. Kasper⁴⁸, I. Katsanos⁶⁵, R. Kehoe⁷⁸, S. Kermiche¹⁵, N. Khalatyan⁴⁸, A. Khanov⁷⁵, A. Kharchilava⁶⁸, Y.N. Kharzhev³⁶, D. Khatidze⁷⁶, M.H. Kirby⁵¹, M. Kirsch²¹, J.M. Kohli²⁷, A.V. Kozelov³⁹, J. Kraus⁶³, A. Kumar⁶⁸, A. Kupco¹¹, T. Kurča²⁰, V.A. Kuzmin³⁸, J. Kvita⁹, S. Lammers⁵², G. Landsberg⁷⁶, P. Lebrun²⁰, H.S. Lee³¹, W.M. Lee⁴⁸, J. Lellouch¹⁷, L. Li⁴⁶, Q.Z. Li⁴⁸, S.M. Lietti⁵, J.K. Lim³¹, D. Lincoln⁴⁸, J. Linnemann⁶³, V.V. Lipaev³⁹, R. Lipton⁴⁸, Y. Liu⁷, Z. Liu⁶, A. Lobodenko⁴⁰, M. Lokajicek¹¹, P. Love⁴², H.J. Lubatti⁸¹, R. Luna-Garcia^{33,e}, A.L. Lyon⁴⁸, A.K.A. Maciel², D. Mackin⁷⁹, R. Madar¹⁸, R. Magaña-Villalba³³, P.K. Mal⁴⁵, S. Malik⁶⁵, V.L. Malyshev³⁶, Y. Maravin⁵⁷, J. Martínez-Ortega³³, R. McCarthy⁷¹, C.L. McGivern⁵⁶, M.M. Meijer³⁵, A. Melnitchouk⁶⁴, D. Menezes⁵⁰, P.G. Mercadante⁴, M. Merkin³⁸, A. Meyer²¹, J. Meyer²³, N.K. Mondal²⁹, T. Moulik⁵⁶, G.S. Muanza¹⁵, M. Mulhearn⁸⁰, E. Nagy¹⁵, M. Naimuddin²⁸, M. Narain⁷⁶, R. Nayyar²⁸, H.A. Neal⁶², J.P. Negret⁸, P. Neustroev⁴⁰, H. Nilsen²², S.F. Novaes⁵, T. Nunnemann²⁵, G. Obrant⁴⁰, D. Onoprienko⁵⁷, J. Orduna³³, N. Osman⁴³, J. Osta⁵⁴, G.J. Otero y Garzón¹, M. Owen⁴⁴, M. Padilla⁴⁶, M. Pangilinan⁷⁶, N. Parashar⁵³, V. Parihar⁷⁶, S.-J. Park²³, S.K. Park³¹, J. Parsons⁶⁹, R. Partridge^{76,c}, N. Parua⁵², A. Patwa⁷², B. Penning⁴⁸, M. Perfilov³⁸, K. Peters⁴⁴, Y. Peters⁴⁴, G. Petrillo⁷⁰, P. Pétroff¹⁶, R. Piegaia¹, J. Piper⁶³, M.-A. Pleier⁷², P.L.M. Podesta-Lerma^{33,f}, V.M. Podstavkov⁴⁸, M.-E. Pol², P. Polozov³⁷, A.V. Popov³⁹, M. Prewitt⁷⁹, D. Price⁵², S. Protopopescu⁷², J. Qian⁶², A. Quadt²³, B. Quinn⁶⁴, M.S. Rangel¹⁶, K. Ranjan²⁸, P.N. Ratoff⁴², I. Razumov³⁹, P. Renkel⁷⁸, P. Rich⁴⁴, M. Rijssenbeek⁷¹, I. Ripp-Baudot¹⁹, F. Rizatdinova⁷⁵, M. Rominsky⁴⁸, C. Royon¹⁸, P. Rubinov⁴⁸, R. Ruchti⁵⁴, G. Safronov³⁷, G. Sajot¹⁴, A. Sánchez-Hernández³³, M.P. Sanders²⁵, B. Sanghi⁴⁸, G. Savage⁴⁸, L. Sawyer⁵⁸, T. Scanlon⁴³, D. Schaile²⁵, R.D. Schamberger⁷¹, Y. Scheglov⁴⁰, H. Schellman⁵¹,

T. Schliephake²⁶, S. Schlobohm⁸¹, C. Schwanenberger⁴⁴, R. Schwienhorst⁶³, J. Sekaric⁵⁶, H. Severini⁷⁴, E. Shabalina²³, V. Shary¹⁸, A.A. Shchukin³⁹, R.K. Shivpuri²⁸, V. Simak¹⁰, V. Sirotenko⁴⁸, P. Skubic⁷⁴, P. Slattery⁷⁰, D. Smirnov⁵⁴, G.R. Snow⁶⁵, J. Snow⁷³, S. Snyder⁷², S. Söldner-Rembold⁴⁴, L. Sonnenschein²¹, A. Sopczak⁴², M. Sosebee⁷⁷, K. Soustruznik⁹, B. Spurlock⁷⁷, J. Stark¹⁴, V. Stolin³⁷, D.A. Stoyanova³⁹, M.A. Strang⁶⁸, E. Strauss⁷¹, M. Strauss⁷⁴, R. Ströhmer²⁵, D. Strom⁴⁹, L. Stutte⁴⁸, P. Svoisky³⁵, M. Takahashi⁴⁴, A. Tanasijczuk¹, W. Taylor⁶, B. Tiller²⁵, M. Titov¹⁸, V.V. Tokmenin³⁶, D. Tsybychev⁷¹, B. Tuchming¹⁸, C. Tully⁶⁷, P.M. Tuts⁶⁹, R. Unalan⁶³, L. Uvarov⁴⁰, S. Uvarov⁴⁰, S. Uzunyan⁵⁰, R. Van Kooten⁵², W.M. van Leeuwen³⁴, N. Varelas⁴⁹, E.W. Varnes⁴⁵, I.A. Vasilyev³⁹, P. Verdier²⁰, L.S. Vertogradov³⁶, M. Verzocchi⁴⁸, M. Vesterinen⁴⁴, D. Vilanova¹⁸, P. Vint⁴³, P. Vokac¹⁰, H.D. Wahl⁴⁷, M.H.L.S. Wang⁷⁰, J. Warchol⁵⁴, G. Watts⁸¹, M. Wayne⁵⁴, G. Weber²⁴, M. Weber^{48,g}, M. Wetstein⁵⁹, A. White⁷⁷, D. Wicke²⁴, M.R.J. Williams⁴², G.W. Wilson⁵⁶, S.J. Wimpenny⁴⁶, M. Wobisch⁵⁸, D.R. Wood⁶¹, T.R. Wyatt⁴⁴, Y. Xie⁴⁸, C. Xu⁶², S. Yacoub⁵¹, R. Yamada⁴⁸, W.-C. Yang⁴⁴, T. Yasuda⁴⁸, Y.A. Yatsunenkov³⁶, Z. Ye⁴⁸, H. Yin⁷, K. Yip⁷², H.D. Yoo⁷⁶, S.W. Youn⁴⁸, J. Yu⁷⁷, S. Zelitch⁸⁰, T. Zhao⁸¹, B. Zhou⁶², N. Zhou⁶⁹, J. Zhu⁷¹, M. Zielinski⁷⁰, D. Zieminska⁵², and L. Zivkovic⁶⁹

(The DØ Collaboration)

¹Universidad de Buenos Aires, Buenos Aires, Argentina

²LAFEX, Centro Brasileiro de Pesquisas Físicas, Rio de Janeiro, Brazil

³Universidade do Estado do Rio de Janeiro, Rio de Janeiro, Brazil

⁴Universidade Federal do ABC, Santo André, Brazil

⁵Instituto de Física Teórica, Universidade Estadual Paulista, São Paulo, Brazil

⁶Simon Fraser University, Burnaby, British Columbia,

Canada; and York University, Toronto, Ontario, Canada

⁷University of Science and Technology of China, Hefei, People's Republic of China

⁸Universidad de los Andes, Bogotá, Colombia

⁹Charles University, Faculty of Mathematics and Physics,

Center for Particle Physics, Prague, Czech Republic

¹⁰Czech Technical University in Prague, Prague, Czech Republic

¹¹Center for Particle Physics, Institute of Physics,

Academy of Sciences of the Czech Republic, Prague, Czech Republic

¹²Universidad San Francisco de Quito, Quito, Ecuador

¹³LPC, Université Blaise Pascal, CNRS/IN2P3, Clermont, France

¹⁴LPSC, Université Joseph Fourier Grenoble 1, CNRS/IN2P3,

Institut National Polytechnique de Grenoble, Grenoble, France

¹⁵CPPM, Aix-Marseille Université, CNRS/IN2P3, Marseille, France

¹⁶LAL, Université Paris-Sud, IN2P3/CNRS, Orsay, France

¹⁷LPNHE, Universités Paris VI and VII, CNRS/IN2P3, Paris, France

¹⁸CEA, Irfu, SPP, Saclay, France

¹⁹IPHC, Université de Strasbourg, CNRS/IN2P3, Strasbourg, France

²⁰IPNL, Université Lyon 1, CNRS/IN2P3, Villeurbanne, France and Université de Lyon, Lyon, France

²¹III. Physikalisches Institut A, RWTH Aachen University, Aachen, Germany

²²Physikalisches Institut, Universität Freiburg, Freiburg, Germany

²³II. Physikalisches Institut, Georg-August-Universität Göttingen, Göttingen, Germany

²⁴Institut für Physik, Universität Mainz, Mainz, Germany

²⁵Ludwig-Maximilians-Universität München, München, Germany

²⁶Fachbereich Physik, University of Wuppertal, Wuppertal, Germany

²⁷Panjab University, Chandigarh, India

²⁸Delhi University, Delhi, India

²⁹Tata Institute of Fundamental Research, Mumbai, India

³⁰University College Dublin, Dublin, Ireland

³¹Korea Detector Laboratory, Korea University, Seoul, Korea

³²SungKyunKwan University, Suwon, Korea

³³CINVESTAV, Mexico City, Mexico

³⁴FOM-Institute NIKHEF and University of Amsterdam/NIKHEF, Amsterdam, The Netherlands

³⁵Radboud University Nijmegen/NIKHEF, Nijmegen, The Netherlands

³⁶Joint Institute for Nuclear Research, Dubna, Russia

³⁷Institute for Theoretical and Experimental Physics, Moscow, Russia

³⁸Moscow State University, Moscow, Russia

³⁹Institute for High Energy Physics, Protvino, Russia

⁴⁰Petersburg Nuclear Physics Institute, St. Petersburg, Russia

⁴¹Stockholm University, Stockholm, Sweden, and Uppsala University, Uppsala, Sweden

- ⁴²Lancaster University, Lancaster LA1 4YB, United Kingdom
⁴³Imperial College London, London SW7 2AZ, United Kingdom
⁴⁴The University of Manchester, Manchester M13 9PL, United Kingdom
⁴⁵University of Arizona, Tucson, Arizona 85721, USA
⁴⁶University of California Riverside, Riverside, California 92521, USA
⁴⁷Florida State University, Tallahassee, Florida 32306, USA
⁴⁸Fermi National Accelerator Laboratory, Batavia, Illinois 60510, USA
⁴⁹University of Illinois at Chicago, Chicago, Illinois 60607, USA
⁵⁰Northern Illinois University, DeKalb, Illinois 60115, USA
⁵¹Northwestern University, Evanston, Illinois 60208, USA
⁵²Indiana University, Bloomington, Indiana 47405, USA
⁵³Purdue University Calumet, Hammond, Indiana 46323, USA
⁵⁴University of Notre Dame, Notre Dame, Indiana 46556, USA
⁵⁵Iowa State University, Ames, Iowa 50011, USA
⁵⁶University of Kansas, Lawrence, Kansas 66045, USA
⁵⁷Kansas State University, Manhattan, Kansas 66506, USA
⁵⁸Louisiana Tech University, Ruston, Louisiana 71272, USA
⁵⁹University of Maryland, College Park, Maryland 20742, USA
⁶⁰Boston University, Boston, Massachusetts 02215, USA
⁶¹Northeastern University, Boston, Massachusetts 02115, USA
⁶²University of Michigan, Ann Arbor, Michigan 48109, USA
⁶³Michigan State University, East Lansing, Michigan 48824, USA
⁶⁴University of Mississippi, University, Mississippi 38677, USA
⁶⁵University of Nebraska, Lincoln, Nebraska 68588, USA
⁶⁶Rutgers University, Piscataway, New Jersey 08855, USA
⁶⁷Princeton University, Princeton, New Jersey 08544, USA
⁶⁸State University of New York, Buffalo, New York 14260, USA
⁶⁹Columbia University, New York, New York 10027, USA
⁷⁰University of Rochester, Rochester, New York 14627, USA
⁷¹State University of New York, Stony Brook, New York 11794, USA
⁷²Brookhaven National Laboratory, Upton, New York 11973, USA
⁷³Langston University, Langston, Oklahoma 73050, USA
⁷⁴University of Oklahoma, Norman, Oklahoma 73019, USA
⁷⁵Oklahoma State University, Stillwater, Oklahoma 74078, USA
⁷⁶Brown University, Providence, Rhode Island 02912, USA
⁷⁷University of Texas, Arlington, Texas 76019, USA
⁷⁸Southern Methodist University, Dallas, Texas 75275, USA
⁷⁹Rice University, Houston, Texas 77005, USA
⁸⁰University of Virginia, Charlottesville, Virginia 22901, USA and
⁸¹University of Washington, Seattle, Washington 98195, USA

(Dated: April 11, 2010)

Using 5.4 fb^{-1} of integrated luminosity from $p\bar{p}$ collisions at $\sqrt{s} = 1.96 \text{ TeV}$ collected by the D0 detector at the Fermilab Tevatron Collider, we search for decays of the lightest Kaluza-Klein mode of the graviton in the Randall-Sundrum model to ee and $\gamma\gamma$. We set 95% C.L. lower limits on the mass of the lightest graviton between 560 and 1050 GeV for values of the coupling k/M_{Pl} between 0.01 and 0.1.

PACS numbers: 13.85.Rm, 11.25.Wx, 14.70.Kv, 14.80.Rt

The large disparity between the scale of quantum gravity, i.e., the Planck scale, $M_{\text{Pl}} \approx 10^{16} \text{ TeV}$, and the electroweak scale, of the order of 1 TeV, is known in the standard model (SM) as the hierarchy problem. In the presence of this hierarchy of scales it is not possible to stabilize the Higgs boson mass at the low values required by experimental data, unless by using an unlikely large amount of fine-tuning.

In the Randall-Sundrum model [1], the existence of a fifth dimension with a warped spacetime metric is proposed, bounded by two three-dimensional branes. The SM fields are localized on one brane, while gravity orig-

inates on the other. With this configuration, TeV scales are naturally generated from the Planck scale due to a geometrical exponential factor (the ‘‘warp factor’’), $\Lambda_\pi = \bar{M}_{\text{Pl}} \exp(-k\pi r_c)$, if $kr_c \approx 12$, where $\bar{M}_{\text{Pl}} = M_{\text{Pl}}/\sqrt{8\pi}$ is the reduced Planck scale, and k and r_c are the curvature scale and compactification radius of the extra dimension, respectively.

Gravitons are the only particles that propagate in the fifth dimension, and appear as a Kaluza-Klein series [2] of massive excitations (KK gravitons, G) with spin 2, mass splitting of the order of 1 TeV, and a universal coupling to the SM fields. Phenomenologically, it is convenient

to express the two Randall-Sundrum parameters k and r_c in terms of two direct observables: the mass of the lightest excitation, M_1 , and the dimensionless coupling to the SM fields, k/\bar{M}_{Pl} . To address the hierarchy problem without the need for fine-tuning, M_1 should be in the TeV range and $0.01 \leq k/\bar{M}_{\text{Pl}} \leq 0.1$ [3]. KK graviton resonances could be produced in high energy particle collisions and would subsequently decay to pairs of SM fermions or bosons.

In this Letter, we report an inclusive search for the lightest KK graviton in the ee and $\gamma\gamma$ decay channels with the D0 detector at the Fermilab Tevatron Collider, where protons and antiprotons collide at $\sqrt{s} = 1.96$ TeV. KK gravitons would be produced via quark-antiquark annihilation and gluon-gluon fusion processes. For $k/\bar{M}_{\text{Pl}} \leq 0.1$, KK gravitons would appear as narrow resonances in the ee and $\gamma\gamma$ invariant mass spectra, with a natural width much smaller than the resolution of the D0 detector and with a branching fraction for the $\gamma\gamma$ decay mode which is twice that of the decay to ee . Previous D0 searches for KK gravitons have excluded $M_1 < 300$ GeV for $k/\bar{M}_{\text{Pl}} = 0.01$ and $M_1 < 900$ GeV for $k/\bar{M}_{\text{Pl}} = 0.1$ at the 95% C.L. [4]. CDF has recently excluded $M_1 < 889$ GeV for $k/\bar{M}_{\text{Pl}} = 0.1$ at the 95% C.L. [5].

The D0 detector [6, 7] consists of tracking detectors, calorimeters, and a muon spectrometer. The tracking system includes a silicon microstrip tracker close to the beam and a central fiber tracker, both located within a 2 T superconducting solenoidal magnet. The liquid-argon and uranium calorimeters consist of a central section covering pseudorapidities $|\eta| \lesssim 1.1$ and two end cap calorimeters that extend the coverage to $|\eta| \approx 4.2$, where $\eta = -\ln[\tan(\theta/2)]$, and θ is the polar angle with respect to the proton beam direction. The azimuthal angle is denoted by ϕ . The electromagnetic (EM) section of the calorimeters is segmented into four longitudinal layers (EM*i*, $i=1,4$) with transverse segmentation of $\Delta\eta \times \Delta\phi = 0.1 \times 0.1$, except for the more finely segmented EM3 section where it is 0.05×0.05 . A preshower system (CPS) uses plastic scintillators with different orientations located between the solenoid and the cryostat of the central calorimeter and provides precise measurements of the positions of EM showers. The luminosity is measured using plastic scintillator arrays placed in front of the end cap calorimeters. The data sample was collected between July 2002 and June 2009 using triggers requiring at least two clusters of energy deposits in the EM calorimeter and corresponds to an integrated luminosity of $5.4 \pm 0.3 \text{ fb}^{-1}$.

We select events with two EM clusters, each with transverse momentum $p_T > 25$ GeV and $|\eta| < 1.1$, reconstructed in a cone of radius $R = \sqrt{(\Delta\eta)^2 + (\Delta\phi)^2} = 0.4$. The EM clusters are required to have at least 97% of their energy deposited in the EM calorimeter and to have the calorimeter isolation variable $I = [E_{\text{tot}}(0.4) -$

$E_{\text{EM}}(0.2)]/E_{\text{EM}}(0.2) < 0.07$, where $E_{\text{tot}}(R)$ [$E_{\text{EM}}(R)$] is the total [EM] energy in a cone of radius R .

Given the different branching fractions for the $\gamma\gamma$ and ee decays of the KK graviton, plus the fact that the two channels have different backgrounds, the analysis treats the two channels separately to optimize the sensitivity. If both EM clusters in an event are spatially matched to tracker activity, either a reconstructed track or a density of hits in the silicon microstrip tracker and central fiber tracker consistent with that of an electron, the event goes in the ee category. Otherwise, the event is put in the $\gamma\gamma$ category, which contains events with at least one EM cluster failing to match tracker activity. With this definition, about 97% of the selected $G \rightarrow ee$ events are put in the ee category and about 90% of the selected $G \rightarrow \gamma\gamma$ events are put in the $\gamma\gamma$ category.

In the ee category, the two electrons are not required to have opposite charges to avoid the loss due to charge misidentification, and two additional requirements are placed on each EM cluster: (i) the scalar sum of the p_T of all tracks originating from the primary vertex (PV, see below) in an annulus of $0.05 < R < 0.4$ around the cluster, I_{trk} , be less than 2.5 GeV; (ii) the cluster be consistent with the electron shower shape using a χ^2 test and a neural network discriminant [8]. In the $\gamma\gamma$ category, additional requirements are placed on each EM cluster: (i) $I_{trk} < 2.0$ GeV; (ii) the energy-weighted shower width in the $r - \phi$ plane in EM3 be less than 3.7 cm; (iii) the cluster be consistent with the photon shower shape using a neural network discriminant.

Proper reconstruction of the event kinematics requires correct identification of the PV of the hard collision. For events in the ee category, the PV is chosen from the list of vertex candidates as the one with the least probability of being a vertex from a soft $p\bar{p}$ interaction as estimated from the p_T of associated tracks. For the $\gamma\gamma$ category, we use the EM-CPS pointing capability, which reconstructs the axes of EM showers by fitting straight lines to shower positions measured in the four longitudinal calorimeter layers and the CPS. The EM-CPS pointing spatial resolution is 3.7 ± 0.2 cm along the beam axis. If at least one photon candidate is matched to a CPS cluster [9], the vertex consistent with the EM-CPS pointing position is chosen as the PV. For events with no photon candidate having a CPS match or events with inconsistent EM-CPS pointing positions of the two photon candidates, the PV is chosen as the one with the highest number of associated tracks. The PV is required to lie within 60 cm of the geometrical center of the detector along the beam axis. The data include a total of 203586 events (186596 in the ee category and 16990 in the $\gamma\gamma$ category) that satisfy these selection criteria and with the invariant mass of the two EM clusters $M_{ee/\gamma\gamma} > 60$ GeV.

All Monte Carlo samples used in this analysis were generated using PYTHIA [10] with CTEQ6L1 [11] parton distribution functions, and processed through a GEANT-

based [12] simulation of the D0 detector and the same reconstruction software as the data. KK graviton signals in the ee and $\gamma\gamma$ decay channels are simulated over the range of parameters $220 \leq M_1 \leq 1050$ GeV and $0.01 < k/\bar{M}_{\text{Pl}} < 0.1$. The accuracy of the PV association has been studied in KK graviton events, where the PV reconstruction efficiency is $\approx 98\%$, with $\approx 96\%$ ($\approx 93\%$) probability to match the true vertex in the ee ($\gamma\gamma$) channel. The simulated and observed invariant mass spectra are compared in ee and $\gamma\gamma$ categories separately. The dominant irreducible background in the ee final state is due to the Drell-Yan (DY) process, where an ee mass-dependent k factor [13] is applied to correct the PYTHIA spectrum for next-to-next-to-leading order effects. The dominant irreducible background in the $\gamma\gamma$ final state is SM $\gamma\gamma$ production, where PYTHIA $\gamma\gamma$ events are reweighted to reproduce the $\gamma\gamma$ invariant mass spectrum predicted by the next-to-leading-order calculation of DIPHOX [14]. D0 has measured the SM $\gamma\gamma$ differential cross section with respect to the $\gamma\gamma$ invariant mass, and in the range used for this analysis (above 60 GeV) the shape of this distribution from DIPHOX agrees with the data [15]. The leading systematic uncertainty on this background's shape arises from the choices in the scales used in the DIPHOX calculation, and is at the level of 10%. The main instrumental background comes from the misidentification of one or two jets as electrons or photons. The shape of the invariant mass spectrum of this source of events is estimated from data by selecting events with EM clusters that are not consistent with electron or photon showers using the χ^2 test (ee category) or the neural network discriminant ($\gamma\gamma$ category). Other SM backgrounds, due to DY $\tau\tau$, $W + \gamma$, WW , ZZ , WZ , $W + \text{jets}$, and $t\bar{t}$ production, are small and are estimated using PYTHIA Monte Carlo events corrected to account for higher order effects [16–18].

Having obtained the shapes of the invariant mass spectra of the various background sources, the background normalization is determined by fitting the invariant mass spectrum of the data to a superposition of the backgrounds in a low-mass control region ($60 < M_{ee/\gamma\gamma} < 200$ GeV), where KK gravitons have been excluded at the 95% C.L. by previous searches. In the fit, the total number of background events is fixed to the number of events observed in the data, and the contributions from SM $\gamma\gamma$, DY ee , and instrumental background are free parameters, while the other SM backgrounds are normalized to their theoretical cross sections. The fit is performed for the ee and $\gamma\gamma$ categories separately. By varying the criteria to select the instrumental background sample and the fitting range, the uncertainty of the background normalization procedure is estimated at the level of 2% (10%) in the ee ($\gamma\gamma$) category.

Figure 1 shows the measured ee and $\gamma\gamma$ invariant mass spectra from the data, superimposed on the expected backgrounds. The data and predicted background

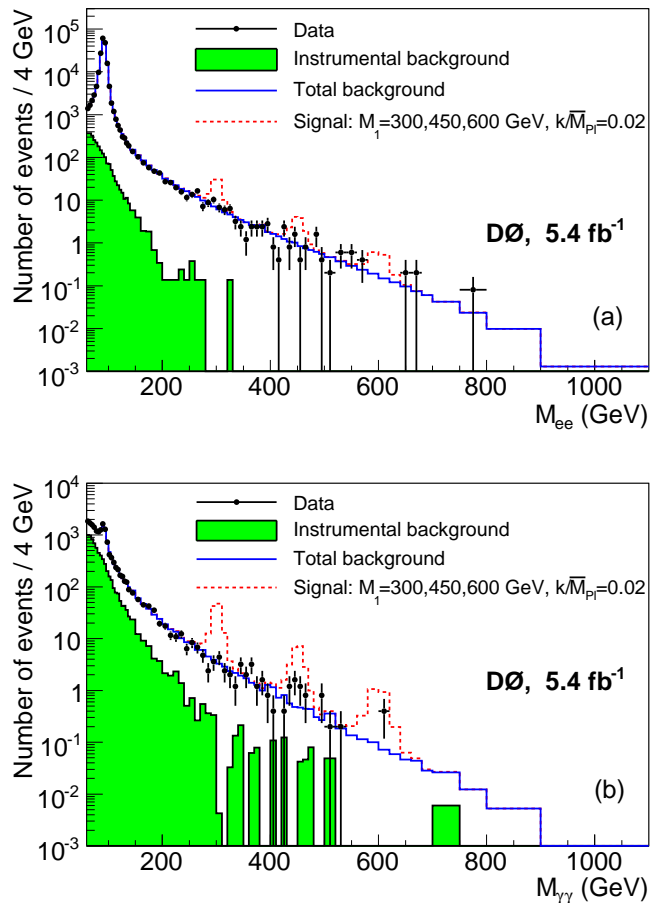


FIG. 1: Invariant mass spectrum from (a) ee and (b) $\gamma\gamma$ data (points). Superimposed are the fitted total background shape from SM processes including instrumental background (open histogram) and the fitted contribution from events with misidentified clusters alone (shaded histogram). The open histogram with dashed line shows the signals expected from KK gravitons with $M_1 = 300, 450, 600$ GeV (from left to right) and $k/\bar{M}_{\text{Pl}} = 0.02$ on top of the total background. Invariant masses below 200 GeV are taken as the control region.

are generally in good agreement. In the region around 450 GeV there is an excess of events in the $\gamma\gamma$ invariant mass spectrum. As estimated with pseudoexperiments, the probability that this excess is exclusively due to backgrounds' fluctuations is 0.011, implying that the background-only hypothesis is disfavored at the 2.30 standard deviations (s.d.) level. If we assume that this excess is due to a KK graviton, including the ee channel reduces the significance to 2.16 s.d..

In the absence of any significant signal for a heavy narrow resonance, we compute upper limits for the production cross section of KK gravitons times the branching fraction into the ee final state using a Poisson log-likelihood ratio (LLR) test [19]. Invariant mass distributions are utilized in the limit calculation. The ee and $\gamma\gamma$ categories are treated as two independent channels,

and then the two separate LLRs are added to obtain a combined exclusion limit assuming the 1:2 ratio of the branching fractions.

Systematic uncertainties on the backgrounds' predictions and on the signal efficiency are considered to calculate limits. These include the integrated luminosity (6.1%), parton distribution functions (0.7% - 6.6% for the acceptance and 9.2% - 16.9% for the graviton production cross section), electron and photon identification efficiency (3.0% per object), EM cluster energy resolution (6%), and trigger efficiency (0.1%). The uncertainty on the acceptance due to initial state radiation (ISR) is estimated to be 4% by varying the parameters governing ISR in PYTHIA. Uncertainties affecting the expected backgrounds arise from electron and photon identification efficiency (3.0% per object), mass dependence of the $DY\ ee$ next-to-next-to-leading order k factor (5.0%), shape of the SM $\gamma\gamma$ invariant mass spectrum, and background normalization. For the EM energy resolution, the SM $\gamma\gamma$ invariant mass spectrum and the background normalization we consider both the effects on the normalization and on the shape of the invariant mass distribution used in extracting limits. For all other systematic sources we consider only changes to the overall background normalization or signal detection efficiency. Systematic uncertainties are incorporated via convolution of the Poisson probability distributions for signal and background with Gaussian distributions corresponding to the different sources of systematic uncertainty. Correlations in the systematic uncertainties between signal and background in ee and $\gamma\gamma$ categories are taken into account.

The resulting limits on the production cross section times branching fraction into electron-positron pairs of the lightest KK graviton, $\sigma(pp \rightarrow G + X) \times B(G \rightarrow ee)$, are given in Table I and displayed in Fig. 2. As shown in Fig. 3, using the cross section predictions from the Randall-Sundrum model with a k factor of 1.54 [20], we can express these results as upper limits on the coupling k/\bar{M}_{Pl} as a function of M_1 .

In summary, using 5.4 fb^{-1} of integrated luminosity collected with the D0 detector at the Fermilab Tevatron Collider, we have searched for a heavy narrow resonance in the ee and $\gamma\gamma$ invariant mass spectra. The observed spectra agree with predictions from SM background processes. For the Randall-Sundrum model with a warped extra dimension, we set 95% C.L. upper limits on $\sigma(pp \rightarrow G + X) \times B(G \rightarrow ee)$ of the lightest Kaluza-Klein mode of the graviton between 6.7 fb and 0.43 fb for masses between 220 and 1050 GeV at the 95% C.L., which translate into lower limits on the mass M_1 of the lightest Kaluza-Klein excitation of the graviton between 560 and 1050 GeV for couplings of the graviton to the SM fields $0.01 \leq k/\bar{M}_{\text{Pl}} \leq 0.1$. These results represent the most sensitive limits to date.

We thank the staffs at Fermilab and collaborating institutions, and acknowledge support from the DOE

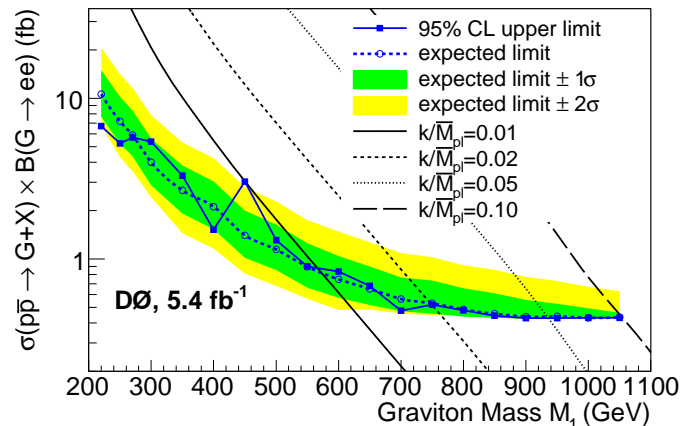


FIG. 2: 95% C.L. upper limit on $\sigma(pp \rightarrow G + X) \times B(G \rightarrow ee)$ from 5.4 fb^{-1} of integrated luminosity compared with the expected limit and the theoretical predictions for different couplings k/\bar{M}_{Pl} .

TABLE I: 95% C.L. upper limit on $\sigma(pp \rightarrow G + X) \times B(G \rightarrow ee)$ and coupling k/\bar{M}_{Pl} from 5.4 fb^{-1} of integrated luminosity.

Graviton Mass GeV	$\sigma \times B(G \rightarrow ee)$ (fb)		Coupling k/\bar{M}_{Pl}	
	Expected	Observed	Expected	Observed
220	10.62	6.71	0.0034	0.0027
250	7.18	5.23	0.0038	0.0033
270	5.91	5.69	0.0042	0.0041
300	4.00	5.37	0.0044	0.0050
350	2.67	3.30	0.0051	0.0056
400	2.12	1.52	0.0062	0.0053
450	1.40	3.03	0.0068	0.0099
500	1.15	1.31	0.0081	0.0087
550	0.89	0.90	0.0093	0.0094
600	0.75	0.84	0.0111	0.0117
650	0.65	0.68	0.0133	0.0136
700	0.56	0.48	0.0160	0.0147
750	0.53	0.52	0.0199	0.0197
800	0.48	0.48	0.0248	0.0247
850	0.46	0.44	0.0316	0.0312
900	0.44	0.43	0.0406	0.0403
950	0.44	0.43	0.0545	0.0539
1000	0.43	0.43	0.0713	0.0713
1050	0.43	0.43	0.0969	0.0964

and NSF (USA); CEA and CNRS/IN2P3 (France); FASI, Rosatom and RFBR (Russia); CNPq, FAPERJ, FAPESP and FUNDUNESP (Brazil); DAE and DST (India); Colciencias (Colombia); CONACyT (Mexico); KRF and KOSEF (Korea); CONICET and UBACyT (Argentina); FOM (The Netherlands); STFC and the Royal Society (United Kingdom); MSMT and GACR (Czech Republic); CRC Program and NSERC (Canada); BMBF and DFG (Germany); SFI (Ireland); The Swedish Research Council (Sweden); and CAS and CNSF (China).

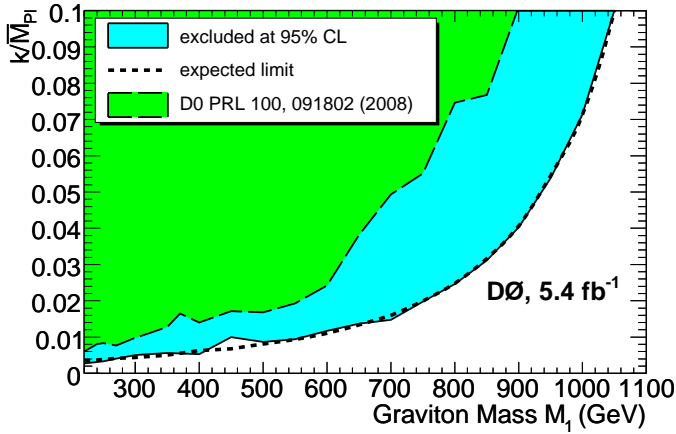


FIG. 3: 95% C.L. upper limit on k/\bar{M}_{Pl} versus the graviton mass M_1 from 5.4 fb^{-1} of integrated luminosity compared with the expected limit and the previously published exclusion contour [4].

-
- [a] Visitor from Augustana College, Sioux Falls, SD, USA.
 [b] Visitor from The University of Liverpool, Liverpool, UK.
 [c] Visitor from SLAC, Menlo Park, CA, USA.
 [d] Visitor from ICREA/IFAE, Barcelona, Spain.
 [e] Visitor from Centro de Investigacion en Computacion - IPN, Mexico City, Mexico.
 [f] Visitor from ECFM, Universidad Autonoma de Sinaloa, Culiacán, Mexico.
 [g] Visitor from Universität Bern, Bern, Switzerland.
-

- [1] L. Randall and R. Sundrum, Phys. Rev. Lett. **83**, 3370 (1999).

- [2] *Modern Kaluza – Klein Theories*, edited by T. Appelquist, A. Chodos, and P. G. O. Freund (Addison-Wesley, Reading, MA, 1987).
 [3] H. Davoudiasl, J. L. Hewett, and T. G. Rizzo, Phys. Rev. Lett. **84**, 2080 (2000); Phys. Rev. D **63**, 075004 (2001).
 [4] D0 Collaboration, V. Abazov *et al.*, Phys. Rev. Lett. **100**, 091802 (2008).
 [5] CDF Collaboration, T. Aaltonen *et al.*, Phys. Rev. Lett. **99**, 0171802 (2007).
 [6] D0 Collaboration, V. Abazov *et al.*, Nucl. Instrum. Methods Phys. Res. A **565**, 463 (2006).
 [7] D0 Collaboration, S. Abachi *et al.*, Nucl. Instrum. Methods Phys. Res. A **338**, 185 (1994).
 [8] D0 Collaboration, V. Abazov *et al.*, Phys. Rev. Lett. **102**, 231801 (2009).
 [9] D0 Collaboration, V. Abazov *et al.*, Phys. Lett. B **659**, 856 (2008).
 [10] T. Sjöstrand *et al.*, Comput. Phys. Commun. **135**, 238 (2001).
 [11] J. Pumplin *et al.*, JHEP **0207** 012 (2002); D. Stump *et al.*, JHEP **0310** 046 (2003).
 [12] R. Brun and F. Carminati, CERN Program Library Long Writeup W5013, 1993 (unpublished).
 [13] R. Hamberg, W. L. van Neerven, and T. Matsuura, Nucl. Phys. **B359**, 343 (1991) [Erratum-ibid. **B644**, 403 (2002)].
 [14] T. Binoth *et al.*, Eur. Phys. J **C16**, 311 (2000).
 [15] D0 Collaboration, V. Abazov *et al.*, arXiv:1002.4917 [hep-ex] (2010), accepted for publication in Phys. Lett. B.
 [16] J. M. Campbell and R. K. Ellis, Phys. Rev. D **60**, 113006 (1999).
 [17] U. Baur and E. L. Berger, Phys. Rev. D **41**, 1476 (1990).
 [18] N. Kidonakis and R. Vogt, Phys. Rev. D **68**, 114014 (2003); M. Cacciari *et al.*, JHEP **04**, 68 (2004).
 [19] W. Fisher, FERMILAB-TM-2386-E (2006).
 [20] P. Mathews *et al.*, JHEP **0510**, 031 (2005).